Alignment of Lysine-Anchored Membrane Peptides under Conditions of Hydrophobic Mismatch: A CD, ^{15}N and ^{31}P Solid-State NMR Spectroscopy Investigation

Ulrike Harzer and Burkhard Bechinger*

Max Planck Institute for Biochemistry, Am Klopferspitz 18A, 82152 Martinsried, Germany

Received April 4, 2000; Revised Manuscript Received July 6, 2000

ABSTRACT: The secondary structure and alignment of hydrophobic model peptides in phosphatidylcholine membranes were investigated as a function of hydrophobic mismatch by CD and oriented proton-decoupled ^{15}N solid-state NMR spectroscopies. In addition, the macroscopic phase and the orientational order of the phospholipid headgroups was analyzed by proton-decoupled ^{31}P NMR spectroscopy. Both, variations in the composition of the polypeptide (10−30 hydrophobic residues) as well as the fatty acid acyl chain of the phospholipid (10−22 carbons) were studied. At lipid-to-peptide ratios of 50, the peptides adopt helical conformations and bilayer macroscopic phases are predominant. The peptide and lipid maintain much of their orientational order even when the peptide is calculated to be 3 Å too short or 14 Å too long to fit into the pure lipid bilayer. A continuous decrease in the ^{15}N chemical shift obtained from transmembrane peptides in oriented membranes suggests an increasing helical tilt angle when the membrane thickness is reduced. This response is, however, insufficient to account for the full hydrophobic mismatch. When the helix is much too long to span the membrane, both the lipid and the peptide order are perturbed, an indication of changes in the macroscopic properties of the membrane. In contrast, sequences that are much too short show little effect on the phospholipid headgroup order, but the peptides exhibit a wide range of orientational distributions predominantly close to parallel to the membrane surface. A thermodynamic formalism is applied to describe the two-state equilibrium between in-plane and transmembrane peptide orientations.

α-Helical domains are important building blocks of membrane proteins, and they also interact with phospholipid bilayers as independent units (reviewed in refs *2* and *3*). In many cases, they adopt transmembrane or in-plane alignments, their orientations depending on a multitude of factors, including their overall hydrophobicity within a membrane-spanning window, the exact length of the hydrophobic region, and the presence of flanking anchoring sequences.

Previous solid-state NMR[1] investigations indicate that charged amphipathic α-helices orient approximately parallel to the membrane surface (*1*, *3*, *4*). In contrast, many hydrophobic sequences assume transmembrane alignments (*1*, *5*−*7*). In addition, hydrophobic helical sequences that are too short to completely span the lipid bilayer in an α-helical conformation such as fusogenic peptides (*8*, *9*) or bacterial signal sequences (*10* and references therein) are also found. These peptides have been shown to adopt oblique alignments or a broad range of topologies.

The role of hydrophobic, polar, and charged amino acids in determining the alignment of α-helical peptides has been investigated using designed amphipathic peptides that carry histidines in the central region of their sequence (*1*, *11*). These peptides change between transmembrane and in-plane orientations in a pH-dependent manner. Their potent antibiotic activity is also a function of pH, and therefore, these peptides allow one to distinguish between several of the suggested models that explain the bacteriocidal activities of these and related peptides (*12*, *13*).

Hydrophobic mismatch has been suggested to be another important determinant for the topology of membrane-associated peptides as well as for the macroscopic phase properties of lipid/peptide mixtures (*14*). Previous investigations show that the phase transition temperatures of phospholipid membranes are modified and new phase transitions are introduced in the presence of high concentrations of model peptides that do not match the hydrophobic thickness of the bilayer (*15*−*18*). Theoretical and experimental studies suggest changes in peptide tilt angle, polypeptide conformational modifications, lipid sorting, peptide aggregation, and phase separations due to hydrophobic mismatch (*14*, *19*−*22*). Such theories are consistent with the observed correlations between membrane protein function and the thickness of lipid bilayers (reviewed in ref *14*). Hydrophobic (mis)match was also suggested to play a role in protein sorting in the endoplasmic reticulum and the Golgi apparatus

* Corresponding author. Telephone: +49 89 8578-2466. Fax: +49 89 8578-2876. E-mail: bechinge@biochem.mpg.de.

[1] Abbreviations: ATR, attenuated total reflection; CD, circular dichroism; DMPC, 1,2-dimyristoyl-*sn*-glycero-3-phosphocholine; DOPC, 1,2-dioleoyl-*sn*-glycero-3-phosphocholine; EPR, electron paramagnetic resonance; FTIR, Fourier transform infrared; HIV, human immunodeficiency virus; HPLC, high-performance liquid chromatography; NMR, nuclear magnetic resonance; PC, 1,2-diacyl-*sn*-glycero-3-phosphocholine; POPC, 1-palmitoyl-2-oleoyl-*sn*-glycero-3-phosphocholine; TFE, trifluoroethanol.

10.1021/bi000770n CCC: $19.00
Published on Web 10/06/2000

or the regulation of membrane protein activity (*23*, *24*). In addition, the hydrophobic core of bacterial signal sequences is too short to completely span the hydrophobic interior of phospholipid bilayers. These peptides, therefore, exhibit unstable topologies which has been suggested to be part of their functional mechanism (*10*).

Solid-state NMR spectroscopy is a powerful method for studying the structure and topology of polypeptides reconstituted into lipid bilayers (reviewed in refs *25*−*28*). In previous investigations, oriented samples of membrane-associated peptides, isotopically labeled with ^{15}N, have been studied by proton-decoupled ^{15}N solid-state NMR spectroscopy. The resulting ^{15}N chemical shift is a sensitive indicator of the approximate membrane alignment of α-helical peptides (*1*). In addition, solid-state NMR spectroscopy has been used to determine the structure of the peptide antibiotics gramicidin (*26*) and magainin 2 (*3*) or the orientational details of the channel-forming viral proteins Vpu of HIV-1 (*7*) and M2 of influenza A (*3*, *6*). Future progress in this type of investigations requires a high degree of sample alignment. A systematic analysis of the orientational distribution of the peptide/lipid samples as a function of the bilayer hydrophobic thickness, therefore, also allows one to better design and adjust experimental parameters during high-resolution solid-state NMR structural studies.

For the investigations presented in this paper, we have synthesized a series of hydrophobic model peptides of the sequence $K_2(LA)_xK_2$ or $K_6L_{20}K_6$ which were subsequently reconstituted into liquid crystalline bilayers composed of symmetric phosphatidylcholines of acyl chains containing 10−22 carbons. Leucine and alanine residues favorably interact with the hydrophobic interior of lipid bilayers; they also show a strong propensity for α-helix formation, in particular in nonpolar environments. Our choice to investigate mixed alanine−leucine sequences was based on previous observations by FTIR spectroscopy on model peptides and on membrane proteins in their natural lipid environment (*16*, *29*). These investigations indicate that infrared spectra of mixed sequences of leucines and alanines compare more favorably to those of natural transmembrane α-helical segments than, for example, polyleucine peptides (*16*). A mixed amino acid composition, therefore, seems to better reflect the surface hydrophobicity and heterogeneity as well as the conformational flexibility of natural polypeptide sequences. The terminal lysines act as membrane surface anchors, and together with the alanines, they help to avoid peptide aggregation during the sample preparations (*18*, *30*, *31*).

Whereas previous solid-state NMR studies have focused on the phospholipid phase behavior as a function of hydrophobic (mis)match in the presence of high concentrations of inserted model peptides (*17*, *18*, *31*), this study investigates in a systematic manner the conformation and alignment of the model peptides themselves as a function of membrane composition. At the same time, the orientational distribution of the phospholipid headgroups in the presence of bilayer-maintaining peptide concentrations is recorded.

MATERIALS AND METHODS

The peptides were prepared by solid phase peptide synthesis on a Millipore 9050 automated peptide synthesizer using Fmoc chemistry. The sequences and their abbreviations used in the text are listed in Table 1. At the underlined positions, ^{15}N-labeled Fmoc-protected amino acid analogues (Promochem, Wesel, Germany) were incorporated. The identity and high purity of the peptides were analyzed by reversed phase HPLC and matrix-assisted laser desorption/ionization mass spectrometry (MALDI-MS).

Table 1: Sequences and Calculated Hydrophobic Lengths of the Peptides Used in This Study

peptide	sequence[a]	calculated hydrophobic length (Å)[b]
hΦ10	KKLAL**A**LALALAKK	15
hΦ16	KKALALALAL**A**LALAALAKK	24
hΦ20	KKLALALALALALAL**A**LALALAKK	30
hΦ25	KKALALALALALALALALAL**A**LALALAKK	37,5
hΦ30	KKLALALALALALALALALALALAL**A**LALALAKK	45
hΦ20L	$K_6L_7\underline{L}L_{12}K_6$	30

[a] **A** is [^{15}N]alanine and $\underline{L}$ [^{15}N]leucine. [b] Assuming 1.5 Å per hydrophobic amino acid.

Oriented samples for solid-state NMR spectroscopy were prepared by dissolving 10−20 mg of peptide in TFE/water mixtures (2 mL/0.3 mL). The pH of the sample was adjusted to neutral by addition of appropriate amounts of 1 N NaOH. Approximately 200 mg of 1,2-diacyl-*sn*-glycero-3-phosphocholine (Avanti Polar Lipids, Birmingham, AL) was added to the sample to yield a lipid-to-peptide ratio of 50. The composition of the fatty acid acyl chains ensured that the phospholipid bilayers are in their liquid crystalline phase at ambient temperature (Table 2). The homogeneous mixtures were applied to 25 thin cover glasses (9 mm × 22 mm), dried slowly, and exposed to high vacuum overnight. After the samples had been equilibrated in an atmosphere of 93% relative humidity for 3 days, the glass plates were stacked on top of each other and sealed. It should be noted that the orientational degree of the phospholipids decreases when the amount of peptide/lipid mixture per area is increased or when the molar ratio of the peptide is increased (*32*). The membrane stacks were inserted into the flat coil of a solid-state NMR probe head with the glass plate normal oriented parallel to the magnetic field direction (*1*). Proton-decoupled ^{15}N solid-state NMR spectra were acquired on a wide-bore Bruker AMX400 or DSX400 spectrometer using a cross-polarization pulse sequence (*33*). The sample was cooled during data acquisition with a stream of air at ambient temperature. Typical acquisition parameters were as follows: spin lock time, 1 ms; recycle delay, 3 s; ^1H B_1-field, 1 mT; 254 data points; and spectral width, 40 kHz. An exponential apodization function corresponding to a line broadening of 400 Hz was applied before Fourier transformation. Chemical shift values are referenced with respect to $(NH_4)_2SO_4$ (27 ppm) and NH_4Cl (41.5 ppm). The "transmembrane part of the peptide" is defined by the ratio of the signal intensity between 150 and 245 ppm over the total signal intensity of the amide bond.

^{31}P solid-state NMR spectra were recorded to analyze the orientational distribution of the phospholipids using a Hahn-echo pulse sequence with proton decoupling (*34*). The ^{31}P 90° pulses ranged in duration from 3.5 to 5.5 μs; the echo

Table 2: Physical Characteristics of the Lipids Used during This Investigation

	phospholipid (abbreviated and full name)	no. of carbons	hydrophobic thickness (Å)	T_m (°C)
DCPC	1,2-dicapryl-*sn*-glycero-3-phosphocholine	10:0	15.5[e]	−32.7[c]
DLPC	1,2-dilauroyl-*sn*-glycero-3-phosphocholine	12:0	19.5[e]	0[a]
	1,2-dimyristoyl-*sn*-glycero-3-phosphocholine	14:1 Δ9cis	20.0[f]	
	1,2-dipalmitoyl-*sn*-glycero-3-phosphocholine	16:1 Δ9cis	23.5[e]	−36[b]
DOPC	1,2-dioleoyl-*sn*-glycero-3-phosphocholine	18:1 Δ9cis	27.0[e]	−14[b]
POPC	1-palmitoyl-2-oleoyl-*sn*-glycero-3-phosphocholine	16:0/18:1 Δ9cis	26.0/27.0[g]	−2[d]
	1,2-dieicosenoyl-*sn*-glycero-3-phosphocholine	20:1 Δ11cis	30.5[f]	
	1,2-dierucoyl-*sn*-glycero-3-ghosphocholine	22:1 Δ13cis	34.0[e]	11[a]

[a] From ref *63*. [b] From ref *64*. [c] From ref *65*. [d] From ref *66*. [e] From ref *67*. [f] Interpolated from shorter and longer lipids using a 1.75 Å C−C bond. [g] The corresponding chain lengths of di-acyl-*sn*-glycerophosphocholines were used (*67*).

delay was 20 μs, and the recycle delay was 3 s. The "undisturbed ^{31}P NMR signal" is defined as the ratio of the intensities of the ^{31}P NMR maximum around 30 ppm when compared to the added signal intensities of the maxima close to 30 and −15 ppm.

Circular dichroism spectra were recorded on an autodichrograph mark IV spectrometer (Jibon-Yvon) in the range of 190−250 nm using quartz cuvettes with a 0.2 mm path length. Ten scans were averaged and corrected for contributions of 1,2-diacyl-*sn*-glycero-3-phosphocholine. The samples used during CD spectroscopy were obtained by adding water to powder-pattern solid-state NMR samples and extrusion through 50 nm polycarbonate filters (Milsch, Laudenbach, Germany). The peptide-to-1,2-diacyl-*sn*-glycero-3-phosphocholine ratio, therefore, was 1/50 (mole/mole) at a peptide concentration of 200−300 μM. The molar ellipticity was calculated using *d*-10-camphorsulfonic acid ($\Theta_{290,5} = 7783$ deg cm^2 dmol^{-1}) as a reference (*35*). CD spectra were analyzed by calculating the ratio of the signals at 222 and 206 nm ($R = \Theta_{222}/\Theta_{206}$) (*36*). This value is independent of peptide concentration and provides a semiquantitative measure of the helical and random coil contributions.

RESULTS

Sequences with a hydrophobic length of 10−30 amino acids were designed to test for the effect of hydrophobic mismatch on the orientation of helical polypeptides as well as on the macroscopic organization of phospholipid bilayers. Whereas alanine and leucine residues form the central core of the sequences, lysines anchor the peptide termini at the membrane interface and increase solubility during sample preparations. Most CD spectra of the peptides in the absence or in the presence of phospholipid bilayers are characterized by strong negative ellipticities at 222 nm, indicating a high degree of helical secondary structure (Figure 1). The results obtained for different peptides with ≥16 hydrophobic amino acids are similar and are in agreement with the high propensity for helix formation of alanine and leucine residues. A significantly lower degree of helical secondary structure is observed for hΦ10. Whereas in aqueous solution this peptide adopts mostly random coil conformations, the relative amount of helix strongly increases in the presence of phospholipid bilayers (Figure 1B).

The proton-decoupled ^{15}N solid-state NMR spectra of ^{15}N-labeled peptides reconstituted into oriented phospholipid bilayers provide a direct measure of the approximate alignment of α-helical polypeptides with respect to the membrane normal (*1*). Whereas a chemical shift value of ∼210 ppm is indicative of transmembrane α-helices, chemical shift values

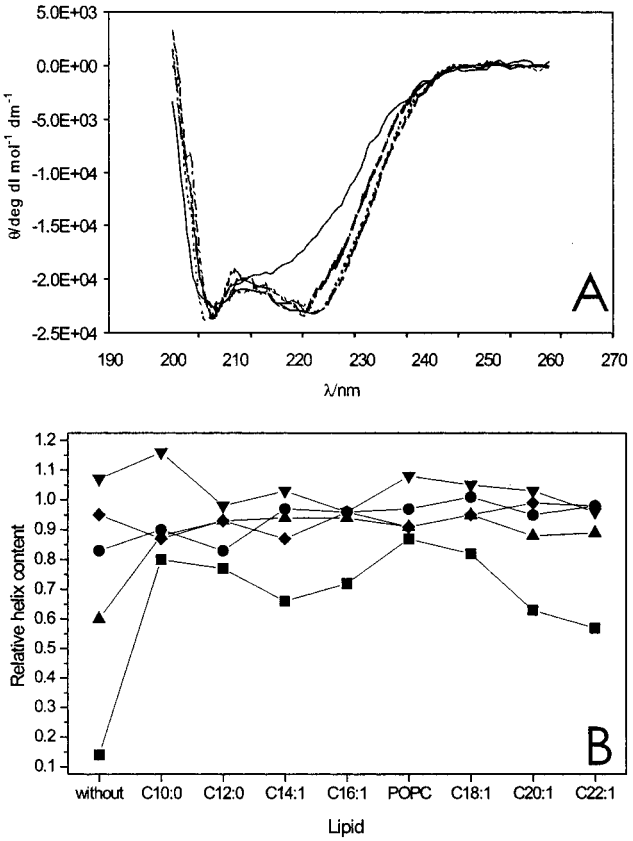

FIGURE 1: (A) Typical CD spectra in the presence of C16:1 PC: hΦ10 (solid line), hΦ16 (hatch-dotted line), hΦ20 (dotted line), hΦ25 (hatched line), and hΦ30 (hatch-double-dotted line). To allow better comparison of the line shapes, a baseline correction using the data between 245 and 260 nm was followed by a scaling of the spectra in such a manner that each spectral minimum matches the one of hΦ10. (B) The relative helix content is shown as a function of lipid composition: hΦ10 (■), hΦ16 (▲), hΦ20 (●), hΦ25 (▼), and hΦ30 (◆). By taking into account statistical and systematic deviations (*68*), we estimated the error of the calculated ratios to be ±0.2.

of <120 ppm are characteristic of helix orientations approximately parallel to the membrane surface. Inspection of panels B−F of Figure 2 indicates that hΦ20 (labeled at the alanine-16 position) exhibits transmembrane orientations when reconstituted into oriented membranes composed of phosphatidylcholine lipids with acyl chains of 12−20 carbon segments. The calculated length of the hydrophobic core of the peptide is 30 Å (Table 1), and the estimated hydrophobic thickness of these membranes is 19.5−30.5 Å (Table 2). Despite considerable deviations between the hydrophobic length of the peptide and the hydrophobic thickness of pure lipid bilayers, transmembrane alignments of the peptide are,

nevertheless, maintained. In contrast, ^{15}N solid-state NMR spectra indicative of a wide range of peptide orientations were observed for hΦ20 when the hydrophobic mismatch between peptides and lipids is augmented further (Figure 2A,G).

By the same principles, proton-decoupled ^{31}P solid-state NMR spectra of liquid crystalline phosphatidylcholine bilayers oriented along glass surfaces exhibit one major resonance around 30 ppm when the phospholipid is aligned with the long axes parallel to the magnetic field direction (i.e., the normal of the glass surface). In contrast, liquid crystalline phosphatidylcholine bilayers that are oriented with their long axes perpendicular to the magnetic field direction resonate at −15 ppm (*37*). However, membrane phospholipids exhibit a high degree of conformational freedom and mobility (*38*, *39*). Changes in the ^{31}P NMR chemical shift are, therefore, indicative of either conformational changes at the lipid headgroup position (*40*), orientational modifications of the lipid molecule as a whole, or both (*37*). On the other hand, the ^{31}P NMR signal is only marginally affected by conformational adjustments of the mobile and flexible acyl chains.

Inspection of Figure 2H−N indicates that the phosphatidylcholine headgroups resonate predominantly at 30 ppm with small contributions between <30 and −15 ppm. Whereas the chemical shift anisotropy of 45 ppm is characteristic of liquid crystalline bilayers as expected from the gel-to-liquid crystalline phase transition temperatures of all phospholipids well below room temperature (Table 2), the position of the main resonance around 30 ppm indicates that the lipid bilayers are well-aligned along the glass surface. The presence of 2 mol % peptide, therefore, does not exhibit pronounced effects on the phospholipid headgroup orientation. Major conformational or orientational readjustments of the phospholipid headgroups are only observed when the hΦ20 peptide is reconstituted into phospholipids with very short (≤12 carbons) or very long (≥20 carbons) fatty acid acyl chains (Figure 2H,I,M,N). When the phospholipid acyl chains are much shorter (10) or much longer (22) than hΦ20, much of the orientational order of both the peptide and the phospholipid is lost and significant signal intensities appear throughout the chemical shift anisotropy of the corresponding ^{15}N and ^{31}P solid-state NMR spectra, respectively (Figure 2A,G,H,N). The broad distribution of signal intensities indicates that different orientations of the phospholipid headgroup and the peptide are in slow exchange on the 10^{-4} s time scale (*1*).

A peptide where all alanines were replaced with leucines (hΦ20L)[2] exhibits a similarly high degree of transmembrane orientation when incorporated into lipid bilayers of intermediate thickness (*32*). This peptide shows a predominant resonance at 215 ppm even when reconstituted into very short or very long acyl chain lipids, thereby contrasting hΦ20. However, the line width of the ^{15}N resonance of the peptide in C10 or C12 lipids is considerably increased when compared with that in long chain PC (*32*).

Hydrophobic mismatch interactions between model peptides of different lengths with phosphatidylcholine membranes of constant hydrophobic thickness were also investigated. In biological membranes, phospholipids with one saturated and one unsaturated acyl chain are often observed. Therefore, POPC is often used to assemble model membrane systems for biophysical investigations. The proton-decoupled ^{15}N and ^{31}P solid-state NMR spectra of hydrophobic model peptides in POPC bilayers as a function of peptide sequence are shown in Figure 3. The hΦ20 peptide matches best the POPC bilayer thickness. Both the ^{15}N and the ^{31}P solid-state NMR spectra are indicative of a high degree of orientation (Figure 3C,H). Deviation from the matching conditions results in an increase in the amount of misaligned peptide (Figure 3A−E). Whereas the amount of ^{31}P NMR signal of the phosphatidylcholine headgroup at −15 ppm remains largely unaffected in the presence of short sequences (Figure 3F,G), considerable orientational and/or conformational disorder is observed in the presence of longer polypeptides (Figure 3I,J).

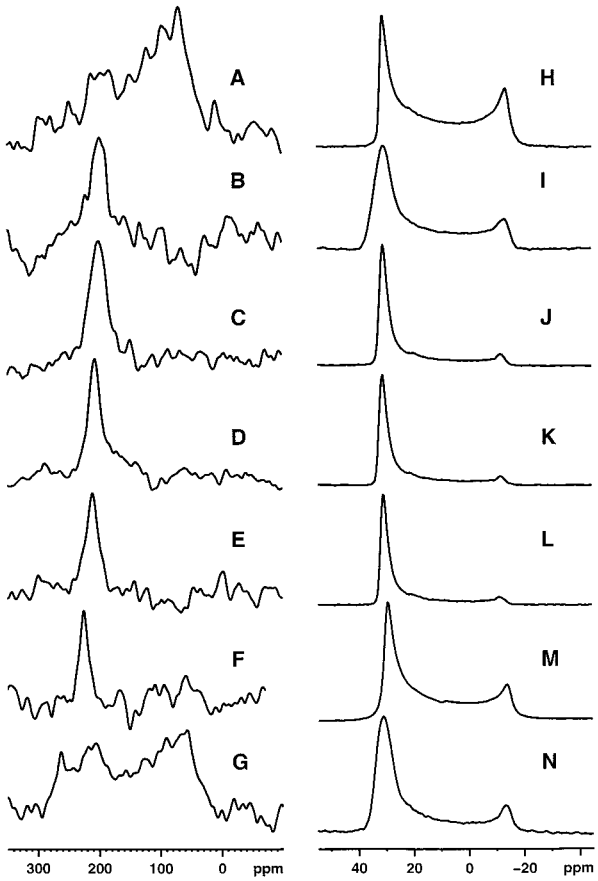

FIGURE 2: Proton-decoupled ^{15}N (A−G) and ^{31}P (H−N) solid-state NMR spectra of hΦ20 reconstituted into diacylphosphatidylcholine membranes of increasing thickness. The membranes were applied onto thin cover glasses for mechanical orientation: (A and H) C10:0, (B and I) C12:0, (C and J) C14:1, (D and K) C16:1, (E and L) C18:1, (F and M) C20:1, and (G and N) C22:1. The spectra were recorded at ambient temperature.

The results shown in Figures 2 and 3 as well as those of additional experiments are summarized in Figures 4 and 5. Figure 4 shows the proportion of integrated ^{15}N signal intensity which is characteristic for transmembrane peptide alignments as a function of fatty acid acyl chain composition. Whereas a wide range of phosphatidylcholines allow a high degree of transmembrane peptide orientation for hΦ16, hΦ20, and hΦ25, signals indicative of membrane-spanning peptides are small or absent in the ^{15}N NMR spectra of hΦ10

[2] Peptides consisting of a core of *n* leucine residues have been named P_n in previous investigations.

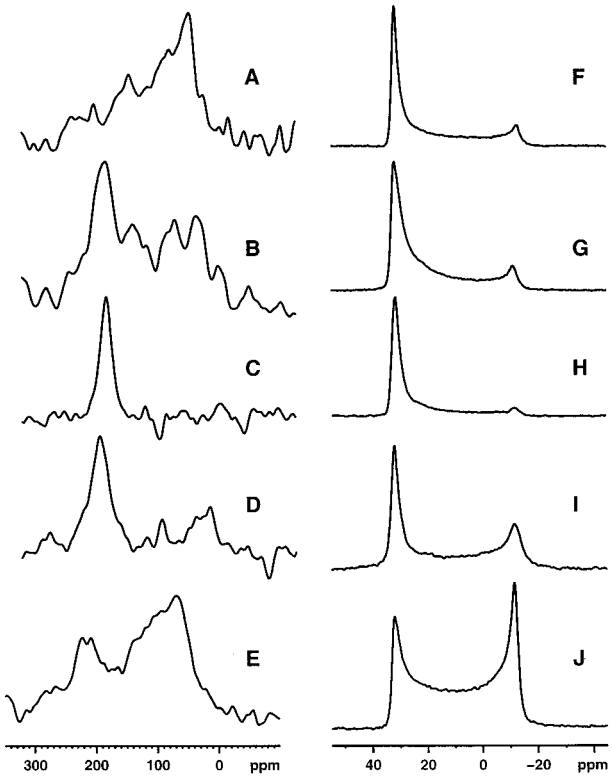

FIGURE 3: Proton-decoupled ^{15}N (A−E) and ^{31}P (F−J) solid-state NMR spectra of peptides of increasing length reconstituted into POPC membranes. The membranes were applied onto thin cover glasses for mechanical orientation: (A and F) hΦ10, (B and G) hΦ16, (C and H) hΦ20, (D and I) hΦ25, and (E and J) hΦ30. The spectra were recorded at ambient temperature.

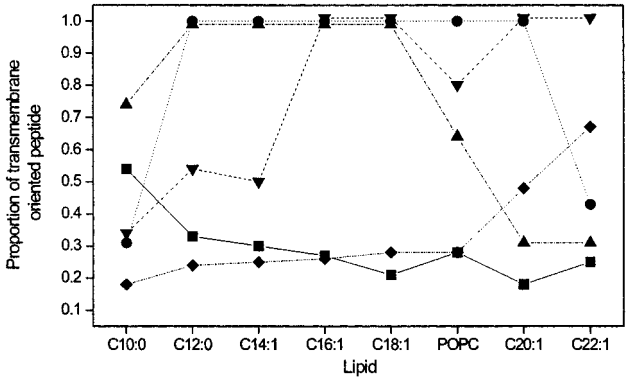

FIGURE 4: Proportion of peptide in a transmembrane orientation as a function of lipid composition: hΦ10 (■), hΦ16 (▲), hΦ20 (●), hΦ25 (▼), and hΦ30 (◆).

and hΦ30. The length of the hΦ30 peptides is, however, reflected in an increase in the transmembrane signal intensity for longer fatty acyl chains. In contrast, hΦ10 exhibits an increase in transmembrane signal intensity upon reduction of the hydrophobic thickness of the membranes. Correspondingly, hΦ25 or hΦ16 exhibit a decreased orientational order when reconstituted into phosphatidylcholines shorter than C16:1 or longer than C18:1, respectively (Figure 4). A high degree of order is also observed in ^{31}P NMR spectra of mechanically supported phosphatidylcholine membranes in the presence of hΦ20 when the fatty acid acyl chains are of intermediate length (Figure 5). Whereas the orientational order of PC membranes is little affected in the presence of hΦ10, a high degree of ^{31}P misalignment is observed in the presence of hΦ30.

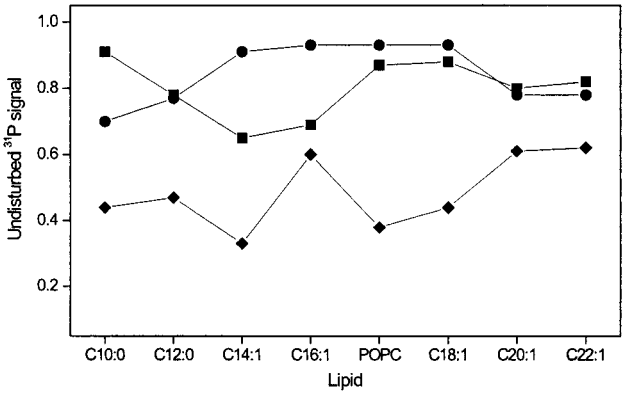

FIGURE 5: Fraction of the undisturbed ^{31}P NMR signal (at approximately 30 ppm) in the presence of 2 mol % peptide: hΦ10 (■), hΦ20 (●), and hΦ30 (◆).

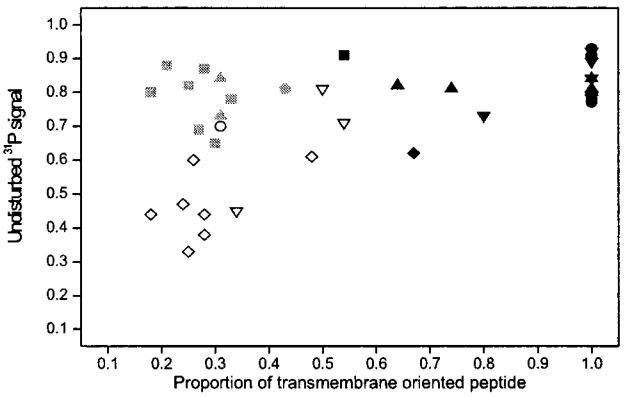

FIGURE 6: Relative amount of unperturbed phospholipid headgroup shown in correlation with the proportion of peptide in a transmembrane orientation: hΦ10 (■), hΦ16 (▲), hΦ20 (●), hΦ25 (▼), and hΦ30 (◆). Black symbols are shown when the hydrophobic thickness of the membrane matches the hydrophobic length of the peptide, gray symbols when the peptide is much too short (mismatch of less than −3 Å), and white symbols when the peptide is much too long (mismatch of more than 14 Å).

When correlations between the well-aligned transmembrane portion of the peptides and the undisturbed ^{31}P NMR signal of the phospholipid headgroups are analyzed, it is possible to distinguish three different cases. First, the hydrophobic thickness of the membrane matches well the hydrophobic length of the peptide. In this case, both the ^{15}N and the ^{31}P NMR spectra are indicative of predominantly transmembrane alignments of peptide and lipid orientations parallel to the glass plate normal, respectively (black symbols in Figure 6). Second, peptides that are too short to span the membrane exhibit orientational distributions with predominantly in-plane alignments. In these samples, the presence of peptide has little effect on the orientational order of the phospholipid membrane (gray symbols). Third, peptides with lengths that exceed the phospholipid bilayer thickness result in broad orientational distributions of both the peptides and the phospholipid headgroups (white symbols).

DISCUSSION

CD and proton-decoupled ^{15}N solid-state NMR spectroscopies indicate that designed hydrophobic peptides consisting of alanines, leucines, and terminal lysine anchors adopt helical conformations in the presence and absence of PC membranes. Only the shortest peptides investigated in

this study exhibit significant random coil contributions. The reasons for this difference can be rationalized in the following manner. First, fraying of the helix termini becomes more important for short peptides. Second, of all the peptides that have been investigated, hΦ10 exhibits the lowest overall helix-forming propensity and the lowest overall hydrophobicity. This peptide is, therefore, expected to exhibit the highest solubility in aqueous buffer and the lowest membrane association constant. This last effect is more important when dilute membrane suspensions are investigated by CD spectroscopy when compared to oriented solid-state NMR samples where bulk water is absent.

When the alignment of peptides with intermediate hydrophobic length is tested by oriented ^{15}N solid-state NMR spectroscopy, they tend to adopt transmembrane alignments. This result is in agreement with previous investigations where these or similar peptides were investigated by oriented X-ray diffraction, ATR-FTIR spectroscopy, or CD spectroscopy (*31*, *41*, *42*). Transmembrane alignments are observed in ^{15}N solid-state NMR spectra even when the calculated thickness of the membrane deviates from the calculated hydrophobic length of an α-helical peptide by ≤3 Å (peptide too short) or ≤14 Å (lipid bilayer too thin). There is, therefore, a high tolerance of biological membranes to adjust to hydrophobic mismatch conditions. In particular, a high degree of adaptation is present when the length of the transmembrane peptide exceeds the thickness of the bilayer. A similar degree of tolerance has also been observed in previous investigations on bilayer-associated polypeptides (*43*, *44*). The underlying mechanisms, which will be discussed further below, might help to keep membrane proteins functional when transported along membranes of cellular compartments with different membrane compositions (*14*).

However, the response to hydrophobic mismatch is not linear. Once the deviation between the length of the peptide and the thickness of the membrane exceeds a given value, the orientational order of mechanically supported lipid bilayers is lost quickly (Figure 4). The peptides and the lipids then adopt orientations different from purely transmembrane (this paper), and/or changes in the macroscopic phases of the membranes are observed (*17*, *45*). Hydrophobic model peptides consisting solely of leucines and alanines as well as two anchoring amino acid residues at each terminus have been shown to induce inverted isotropic or hexagonal II phases in phosphatidylcholine membranes at high peptide concentrations (>3 mol %). These phase transitions exhibit a functional dependence on the amount of hydrophobic mismatch and are more pronounced when the hydrophobic length of the lipid exceeds that of the peptide (*14*, *17*, *31*).

When the hydrophobic length of the peptide and the hydrophobic membrane thickness differ, several means of adaptation have been suggested to take place and to help avoid the exposure of hydrophobic surfaces to the aqueous environment (*14*). In cases where the peptide is too long, the soft surfaces formed by phospholipid bilayers can adapt to some extent to the additional strain imposed by the peptides. Modeling studies indeed indicate large fluctuations (≤10 Å) of the lipid bilayer surface along the membrane normal (*46*−*48*), in addition to elastic interactions and undulations of the lipid bilayer (*49*). Such flexibility could form the basis for local adjustments at the lipid−peptide boundary.

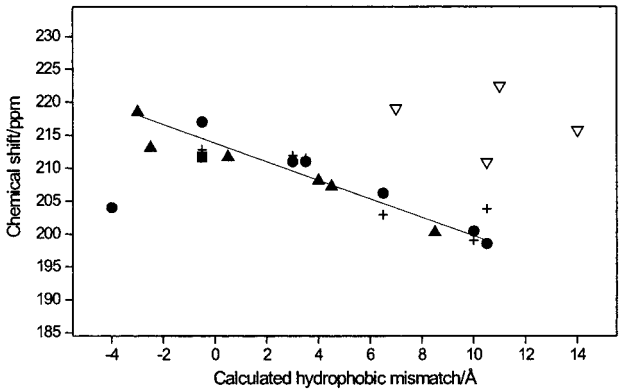

FIGURE 7: ^{15}N chemical shift observed in mechanically oriented membrane samples (normal parallel to the magnetic field direction) as a function of the calculated hydrophobic mismatch. Only samples which exhibit a well-established transmembrane peak are analyzed (with fractions of transmembrane peptide alignment of ≥40%): hΦ10 (■), hΦ16 (▲), hΦ20 (●), hΦ25 (▽), and hΦ20L (+). Please note that the calculated hydrophobic length of the peptide does not take into consideration the hydrophobic extensions of the lysine side chains that increase the effective hydrophobic length of the peptide (*31*).

It has been shown, for example, that the lipid phase transition temperatures and the fatty acid acyl chain ^{2}H-C order parameters increase in the presence of long peptides. Changes in the ^{2}H NMR quadrupolar splittings of deuterated fatty acid acyl chains have been used to calculate the hydrophobic thickness in the presence of increasing peptide concentrations (*18*, *31*, *50*). The reduction in the number of carbon chain gauche conformers results in an increase in bilayer thickness and concomitantly a reduction in lipid surface area. The phospholipid headgroups on the other hand are affected little, if at all, by the presence of 2 mol % peptide and within a limited degree of hydrophobic mismatch (Figures 2J−L and 3F−H). However, when the changes in acyl chain order parameters are analyzed in terms of bilayer thickness, these changes cannot completely account for the full extent of adaptation necessary to avoid exposure of hydrophobic surfaces to polar environments (*18*, *29*, *50*).

It has, therefore, been suggested that increased tilt angles of peptide α-helices result in a decreased effective length of the peptide, thereby reducing hydrophobic mismatch. Indeed, the ^{15}N chemical shifts of well-oriented samples decrease in a systematic manner when the extent of hydrophobic mismatch (peptide too long) increases (Figure 7). Although, in general, a single ^{15}N chemical shift measurement is insufficient to accurately determine the helix tilt angle, the highest ^{15}N chemical shift value measured in this study for clearly transmembrane peptides is, within experimental error, in agreement with a 0° tilt angle (Figures 7 and 8). When all other parameters, such as main tensor elements and the rotational alignment of the peptide around the helix axis, are kept constant, a 26 ppm decrease in chemical shift indicates an increase in the tilt angle of 20°. This situation is described by a merely vertical displacement in Figure 8. Such an increase in tilt angle corresponds to a decrease in the effective length of the helix within the bilayer of 2 Å. When all possible rotation angles around the helix axis as well as experimental errors are taken into consideration, the measured ^{15}N chemical shift values of >195 ppm are in agreement with tilt angles between 0 and <35° (Figure 8). A change in the tilt angle from 0 to <35° shortens the

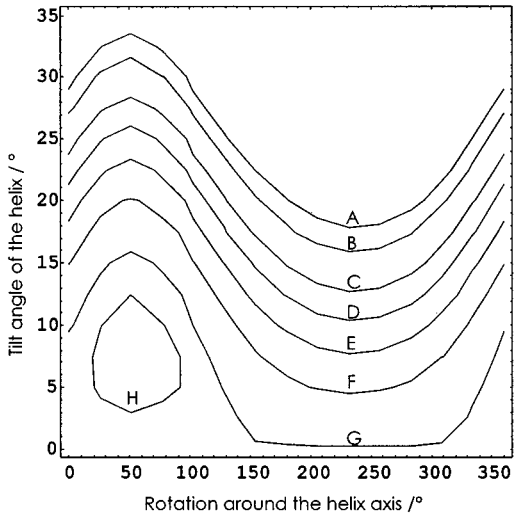

FIGURE 8: Calculation of possible tilt angles of ideal α-helical peptides that are in agreement with the ^{15}N chemical shifts of the transmembrane contribution of aligned samples. α-Helical peptides were rotated in a stepwise manner first around the helix axis and thereafter around a perpendicular axis. For every possible spatial orientation, the chemical shifts were calculated. The contours indicate peptide orientations with chemical shifts of (A) 198, (B) 202, (C) 208, (D) 212, (E) 216, (F) 220, (G) 224, and (H) 226 ppm. The tensor elements that were used (227, 74, and 59 ppm) were evaluated from an experimental powder pattern of hΦ20, and the orientation of the tensor within the molecular coordinate system was according to ref *62*. In the ensemble of hΦ*n*−peptide samples, chemical shift maxima of >227 ppm were absent (e.g., Figures 2−4).

projection of the hΦ20 helix axis onto the bilayer normal by <5.5 Å. Even this value falls short of compensating fully for the calculated hydrophobic mismatch (≥10 Å).

Conformational changes of the peptide backbone could provide further mechanisms for adjusting the length of the peptide to the bilayer hydrophobic thickness and at the same time avoiding unfavorable disruption of the packing of the lipid molecules. In cases where the peptide α-helix is too long, a π-helical conformation can shorten the peptide by about 15%. Long helices at large tilt angles impose considerable strain on the surrounding lipids; therefore, it is interesting to note that bent helices have been observed during molecular modeling calculations (*51*). The peptides hΦ25 and hΦ30 do not follow the same linear chemical shift relationship of the shorter polypeptides (Figure 7), suggesting that these long sequences deviate from a straight helical end-to-end conformation.

To test the possibility of conformational alterations in more detail, the membrane alignment of hΦ20L has also been tested. It has been shown in previous FTIR spectroscopic measurements that leucine−alanine hybrid peptides reconstituted into membranes exhibit considerably higher conformational freedom when compared to polyleucine sequences (*16*, *29*). However, when investigated in oriented lipid membranes, the polyleucine sequence exhibits not only comparable ^{15}N chemical shift values (Figure 7) but also a similar or even wider tolerance to hydrophobic mismatch conditions when compared to hΦ20 (not shown).

When the peptide is too short to match the hydrophobic thickness of the bilayer, the possibility exists that the lipids increase in area and at the same time reduce their length along the bilayer normal. It has been shown, however, that the bilayer disrupts when its area expansion exceeds 2−3% (*52*). Experimental measurements of the lipid acyl chain order parameters indeed indicate that phosphatidylcholines of the first-shell lipids surrounding model peptides increase in length by ≤6.3 Å, but decrease by only ≤1.8 Å (*18*). In addition, snorkelling of charged side chains to the membrane surface (*53*) or α- to 3_{10}-helix transitions (lengthening by 15%) provides some potential for adjustments. Nonhelical conformations can be considered as well. These latter conformations, however, cause the unfavorable exposure of nonsaturated hydrogen bonds within the membrane interior. As a consequence, in the presence of lipid bilayers, a high degree of helicity is observed in CD spectroscopic measurements for all peptides investigated in this work (Figure 1). This technique, however, is not sufficiently sensitive for differentiating between helical conformations.

In contrast, transmembrane-oriented peptides that are too short to span the hydrophobic region of the membrane lack the possibility of adjusting to the bilayer by bending or tilting the helix axis, thereby contrasting the situation when the peptide is too long (cf. above). These limitations in conjunction with the previous discussion explain why long peptides better adjust to hydrophobic mismatch when compared to sequences that are too short (Figures 4 and 6). A similar asymmetry has also been observed when bacteriorhodopsin has been reconstituted in long- or short-chain phospholipids (*43*) or when polyleucine model sequences have been investigated in bilayers with different compositions (*44*, *54*, *55*).

The ^{15}N solid-state NMR spectra of peptides considerably shorter than the hydrophobic thickness of the bilayer indicate a wide distribution of peptide orientations (Figures 2A, 3A, and 6). At the same time, a high degree of order is retained in ^{31}P solid-state NMR spectra (Figures 3 and 6). These observations suggest that an equilibrium situation exists where the peptide tends to fluctuate slowly between in-plane and transmembrane orientations. Similar equilibria have also been observed when the insertion of tryptophan-labeled polyleucine peptides was investigated by fluorescence spectroscopy (*55*) or when the topologies of helices in larger membrane proteins were studied (*56*, *57*). Whereas an in-plane alignment results in exposure of hydrophobic residues to the bilayer interface (*58*), a transmembrane configuration is unstable due to extensive hydrophobic mismatch (exposing hydrophobic areas of the lipids to polar environments). A comparable situation has been observed when the membrane alignment of the M13 coat protein signal sequence has been investigated in POPC membranes (*10*). The architecture of this peptide consisting of an α-helical hydrophobic core region of approximately 12 residues and charged and polar residues at the termini has in fact initiated the study presented here. Although this peptide is immobilized in the presence of lipid membranes, its amide protons remain water accessible in micellar complexes and the peptide helix adopts a wide range of alignments in oriented ^{15}N solid-state NMR spectra (*10*).

To quantitatively describe two-state equilibria between monomeric peptides with in-plane alignments (location at the membrane interface) and transmembrane peptide orientations, a complex set of peptide−bilayer interactions needs to be considered. Whereas previous work from this laboratory has established a formalism that describes this type of

equilibrium (*1*), excellent descriptions of transfer processes between aqueous and interfacial environments (*58*) or between the water phase and the membrane interior have been published (*58*, *59*). Under conditions of hydrophobic mismatch, the transition from interfacial peptide locations to transmembrane configurations is described by the difference in the Gibbs free energy between these states (*1*):

$$\Delta G = \Delta G^{d} + \Delta G^{h} + \Delta G^{p} + \Delta G^{m} + \Delta G^{l} + \Delta G^{W} + \Delta G^{hh} + \Delta G^{\#}$$

This equation takes into consideration the pH-dependent energy of discharge (ΔG^{d}),[3] hydrophobic interactions (ΔG^{h}), energy contributions from placing polar side chains into the hydrophobic interior (ΔG^{p}), hydrophobic mismatch energy (ΔG^{m}), and all other contributions ($\Delta G^{\#}$). If not considered already during the evaluation of ΔG^{m} changes in lipid−lipid interactions such as entropic (lipophobic), van der Waals and headgroup−headgroup interactions ($\Delta G^{l} + \Delta G^{W} + \Delta G^{hh}$) should also be taken into account. We assume that the transition from water to the membrane interface, although important in other experimental setups, is negligible in our solid-state NMR experiments as bulk water is absent in oriented samples hydrated at ≤95% relative humidity. Nevertheless, it should be noted that the potential energy differences of transferring side chains from the polar interface to the hydrophobic membrane interior are considerably reduced when compared to those involved to place an amino acid side chain from bulk water to the membrane interior (*58*). When polyleucine sequences are compared to alanine−leucine hybrid peptides or when PC is exchanged with phosphatidylethanolamines, differences in the hydrophobic mismatch interactions have been observed (*16*, *29*, *32*, *60*). These differences can be attributed at least in part to changes in hydrophobic interactions of the peptide (e.g., ΔG^{h}) or to changes in the lipid−lipid and lipid−peptide interactions ($\Delta G^{l} + \Delta G^{W} + \Delta G^{hh}$). The real situation might, of course, be considerably more complicated with additional equilibria between the in-plane intercalated peptide and the aqueous phase as well as aggregation of peptides in their in-plane, transmembrane, or in-buffer configurations.

Our results suggest that some of the shorter peptides consist of an ensemble of amino acids that is sufficiently hydrophilic for the peptide to reside at the membrane interface. In the case of hΦ10, the unfavorable hydrophobic energy contributions of placing five alanines and five leucines in the membrane interface (ΔG^{h}) is more than compensated by the gain in ΔG^{m} where this location avoids extensive hydrophobic mismatch. Formalisms for describing this latter energy contribution have been developed in previous theoretical studies (*19*, *21*, *22*, *61*). Peptides, when intercalated into the membrane interface, cause a "mismatch" situation in a different sense, as the helix diameter of 10−12 Å is insufficient to fill the depth of, for example, a POPC monolayer completely (*12*). Short peptides, however, occupy a small surface area (ca. 12 Å × 15 Å) and thereby cause a comparatively small local distortion in the lipid bilayer packing. These are easily accommodated by small conformational changes of the lipid fatty acid acyl chains. The in-plane bilayer interactions of small hydrophobic peptides, thereby, resemble to some extent the situation when amphipathic helices such as PGS (magainin) or mastoparan are intercalated into the membrane interface (*12*, *28*).

In contrast, the hydrophobic energy contributions of hΦ25 or hΦ30 are increased 2−3 times when transitions between in-plane and transmembrane orientations are considered. At the same time, the hydrophobic mismatch energy (ΔG^{m}) is similar or smaller in magnitude (cf. the above discussion and refs *19*, *21*, and *61*). As a consequence, these peptides are less likely to be found at the membrane surface. Indeed, both ^{31}P and ^{15}N solid-state NMR spectra are indicative of profound rearrangements in the membrane organization when long hydrophobic sequences cannot be accommodated in a transmembrane fashion due to hydrophobic mismatch. Although these samples, when supported by glass surfaces, do not exhibit a high degree of orientational order (Figure 3E,J), ^{31}P NMR spectra of these or unoriented samples (not shown) are characteristic of liquid crystalline phospholipid bilayers.

The formation of peptide oligomers provides alternative mechanisms of adaptation to hydrophobic mismatch. Oligomerization reduces the contact area between lipids and peptide. From our NMR spectra, we cannot favor or exclude this possibility. However, peptides such as WALP, hΦ23, and P_{24} do not form extended aggregates in the presence of DMPC, DOPC, and POPC membranes, respectively (*18*, *30*, *31*). In addition, electron microscopic studies indicate that bacteriorhodopsin remains monomeric in a wide variety of lipids when reconstituted into model membranes (*43*). On the other hand, red-shifted fluorescence signals at increasing P_{23} concentrations are suggestive of oligomerization in DOPC membranes (*55*).

In summary, this and previous investigations indicate that several major nonlinear mechanisms are active at the same time for mutually adjusting the effective hydrophobic length and/or thickness of peptides and lipids. Under the experimental conditions used in this work, these include changes in lipid and peptide conformations as well as alterations in peptide tilt angle and topology (and possibly aggregation). As large changes of one of these structural factors will create exceedingly high unfavorable energy contributions, the use of several different mechanisms to adjust to hydrophobic mismatch is part of optimizing the potential energy of the system.

ACKNOWLEDGMENT

We are grateful to Bas Vogt and Pieter Jasperse for their critical comments on the manuscript. Bas Vogt also helped during chemical shift tensor calculations and CD spectroscopic measurements. Monika Zobawa, Susan Schinzel, and Martin Grimme provided valuable support during peptide synthesis, HPLC purification, and analysis of the peptide synthetic products by mass spectrometry. We are grateful to Luis Moroder and Dieter Oesterhelt for giving us access to their instrumentation.

[3] Estimates of transfer energies indicate that removal of the charge from an acid and/or base is more favorable when compared to placing a charge within the hydrophobic bilayer interior (*1*). For amino acid *i*, the energy of discharge is calculated according to the equation $\Delta G_i^{d} = RT \ln r + 2.3RT(pK_i - pH)$, where *r* is the minimal ratio of uncharged-to-charged side chains that is acceptable for a location in the bilayer interior ($r > 90$) and *R*, *T*, pH, and p*K* have their usual meaning.

REFERENCES

1. Bechinger, B. (1996) *J. Mol. Biol. 263*, 768−775.
2. Garavito, R. M. (1998) *Curr. Opin. Struct. Biol. 9*, 344−349.
3. Bechinger, B., Kinder, R., Helmle, M., Vogt, T. B., Harzer, U., and Schinzel, S. (1999) *Biopolymers 51*, 174−190.
4. Mattila, K., Kinder, R., and Bechinger, B. (1999) *Biophys. J. 77*, 2102−2113.
5. North, C. L., Barranger-Mathys, M., and Cafiso, D. S. (1995) *Biophys. J. 69*, 2392−2397.
6. Kovacs, F. A., and Cross, T. A. (1997) *Biophys. J. 73*, 2511−2517.
7. Wray, V., Kinder, R., Federau, T., Henklein, P., Bechinger, B., and Schubert, U. (1999) *Biochemistry 38*, 5272−5282.
8. Voneche, V., Portetelle, D., Kettmann, R., Willems, L., Limbach, K., Paoletti, E., Ruysschaert, J. M., Burny, A., and Brasseur, R. (1992) *Proc. Natl. Acad. Sci. U.S.A. 89*, 3810−3814.
9. Martin, I., Schaal, H., Scheid, A., and Ruysschaert, J. M. (1996) *J. Virol. 70*, 298−304.
10. Bechinger, B. (1997) *Proteins: Struct., Funct., Genet. 27*, 481−492.
11. Bechinger, B., Ruysschaert, J. M., and Goormaghtigh, E. (1999) *Biophys. J. 76*, 552−563.
12. Bechinger, B. (1997) *J. Membr. Biol. 156*, 197−211.
13. Vogt, T. C. B., and Bechinger, B. (1999) *J. Biol. Chem. 274*, 29115−29121.
14. Killian, J. A. (1998) *Biochim. Biophys. Acta 1376*, 401−416.
15. Huschilt, J. C., Hodges, R. S., and Davis, J. H. (1985) *Biochemistry 24*, 1377−1386.
16. Zhang, Y. P., Ruthven, N. A. H. L., Hodges, R., and McElhaney, R. N. (1995) *Biochemistry 34*, 2362−2371.
17. Killian, J. A., Salemink, I., de Planque, M. R. R., Lindblom, G., Koeppe, R. E., II, and Greathouse, D. V. (1996) *Biochemistry 35*, 1037−1045.
18. de Planque, M. R., Greathouse, D. V., Koeppe, R. E., II, Schafer, H., Marsh, D., and Killian, J. A. (1998) *Biochemistry 37*, 9333−9345.
19. Owicki, J. C., Springgate, M. W., and McConnell, H. M. (1978) *Proc. Natl. Acad. Sci. U.S.A. 75*, 1616−1619.
20. Mouritsen, O. G., and Bloom, M. (1984) *Biophys. J. 46*, 141−153.
21. Fattal, D. R., and Ben-Shaul, A. (1993) *Biophys. J. 65*, 1795−1809.
22. May, S., and Ben-Shaul, A. (1999) *Biophys. J. 76*, 751−767.
23. Bretscher, M. S., and Munro, S. (1993) *Science 261*, 1280−1281.
24. Masibay, A. S., Balaji, P. V., Boeggeman, E. F., and Qasba, P. K. (1993) *J. Biol. Chem. 268*, 9908−9916.
25. McDowell, L. M., and Schaefer, J. (1996) *Curr. Opin. Struct. Biol. 6*, 624−629.
26. Cross, T. A. (1997) *Methods Enzymol. 289*, 672−696.
27. Griffin, R. G. (1998) *Nat. Struct. Biol. (NMR Suppl.)*, 508−512.
28. Bechinger, B. (1999) *Biochim. Biophys. Acta 1462*, 157−183.
29. Zhang, Y. P., Ruthven, N. A. H. L., Hodges, R. S., and McElhaney, R. N. (1992) *Biochemistry 31*, 11579−11588.
30. Subczynski, W. K., Lewis, R. N., McElhaney, R. N., Hodges, R. S., Hyde, J. S., and Kusumi, A. (1998) *Biochemistry 37*, 3156−3164.
31. Zakharov, S. D., Lindeberg, M., and Cramer, W. A. (1999) *Biochemistry 38*, 11325−11332.
32. Harzer, U. (2000) Ph.D. Thesis, Technical University Munich, Munich.
33. Pines, A., Gibby, M. G., and Waugh, J. S. (1973) *J. Chem. Phys. 59*, 569−590.
34. Rance, M., and Byrd, R. A. (1983) *J. Magn. Reson. 52*, 221−240.
35. Chen, G. C., and Yang, J. T. (1977) *Anal. Lett. 10*, 1195−1207.
36. Bruch, M. D., Dhingra, M. M., and Gierasch, L. M. (1991) *Proteins: Struct., Funct., Genet. 10*, 130−139.
37. Seelig, J. (1978) *Biochim. Biophys. Acta 515*, 105−140.
38. Seelig, J. (1977) *Q. Rev. Biophys. 10*, 353−418.
39. Huster, D., Arnold, K., and Gawrisch, K. (1999) *J. Phys. Chem. B 103*, 243−251.
40. Seelig, J., Macdonald, P. M., and Scherer, P. G. (1987) *Biochemistry 26*, 7535−7541.
41. Huschilt, J. C., Millman, B. M., and Davis, J. H. (1989) *Biochim. Biophys. Acta 979*, 139−141.
42. Axelsen, P. H., Kaufman, B. K., McElhaney, R. N., and Lewis, R. N. (1995) *Biophys. J. 69*, 2770−2781.
43. Lewis, B. A., and Engelman, D. M. (1983) *J. Mol. Biol. 166*, 203−210.
44. Webb, R. J., East, J. M., Sharma, R. P., and Lee, A. G. (1998) *Biochemistry 37*, 673−679.
45. Morein, S., Strandberg, E., Killian, J. A., Persson, S., Arvidson, G., Koeppe, R. E., II, and Lindblom, G. (1997) *Biophys. J. 73*, 3078−3088.
46. Tieleman, D. P., Marrink, S. J., and Berendsen, H. J. (1997) *Biochim. Biophys. Acta 1331*, 235−270.
47. Berneche, S., Nina, M., and Roux, B. (1998) *Biophys. J. 75*, 1603−1618.
48. Feller, S. E., Huster, D., and Gawrisch, K. (1999) *J. Am. Chem. Soc. 121*, 8963−8964.
49. Sackmann, E. (1994) *FEBS Lett. 346*, 3−16.
50. Nezil, F. A., and Bloom, M. (1992) *Biophys. J. 61*, 1176−1183.
51. Belohorcova, K., Davis, J. H., Woolf, T. B., and Roux, B. (1997) *Biophys. J. 73*, 3039−3055.
52. Kwok, R., and Evans, E. (1981) *Biophys. J. 35*, 637−652.
53. Segrest, J. P., De Loof, H., Dohlmann, J. G., Brouillette, C. G., and Anatharamaiah, G. M. (1990) *Proteins: Struct., Funct., Genet. 8*, 103−117.
54. Ren, J., Lew, S., Wang, Z., and London, E. (1997) *Biochemistry 36*, 10213−10220.
55. Ren, J., Lew, S., Wang, J., and London, E. (1999) *Biochemistry 38*, 5905−5912.
56. Kienker, P. K., Qiu, X., Slatin, S. L., Finkelstein, A., and Jakes, K. S. (1997) *J. Membr. Biol. 157*, 27−37.
57. Lambotte, S., Jasperse, P., and Bechinger, B. (1998) *Biochemistry 37*, 16−22.
58. White, S. H., and Wimley, W. C. (1999) *Annu. Rev. Biophys. Biomol. Struct. 28*, 319−365.
59. Engelman, D. M., Steitz, T. A., and Goldman, A. (1986) *Annu. Rev. Biophys. Biophys. Chem. 15*, 321−353.
60. Zhang, Y. P., Lewis, R. N., Hodges, R. S., and McElhaney, R. N. (1995) *Biophys. J. 68*, 847−857.
61. Mouritsen, O. G., and Bloom, M. (1984) *Biophys. J. 46*, 141−150.
62. Lazo, N. D., Hu, W., and Cross, T. A. (1995) *J. Magn. Reson. 107*, 43−50.
63. Caffrey, M., and Feigenson, G. W. (1981) *Biochemistry 20*, 1949−1961.
64. Van Dijck, P. W., De Kruijff, B., Van Deenen, L. L., de Gier, J., and Demel, R. A. (1976) *Biochim. Biophys. Acta 455*, 576−587.
65. Huang, C., Wang, Z. Q., Lin, H. N., Brumbaugh, E. E., and Li, S. (1994) *Biochim. Biophys. Acta 1189*, 7−12.
66. Silvius, J. R. (1982) *Thermotropic Phase Transitions of Pure Lipids in Model Membranes and Their Modifications by Membrane Proteins*, John Wiley and Sons, New York.
67. Lewis, B. A., and Engelman, D. M. (1983) *J. Mol. Biol. 166*, 211−217.
68. Wooley, A. G., and Wallace, B. A. (1993) *Biochemistry 32*, 9819−9825.

BI000770N